Innovative Infrastructure Solutions (2024) 9:239
https://doi.org/10.1007/s41062-024-01542-1

TECHNICAL PAPER

Evaluation of seismic bearing capacity of strip footing on soil slope using finite element limit analysis

Nimisha Dwivedi[1] · Vinay Bhushan Chauhan[1]

Received: 21 June 2021 / Accepted: 16 May 2024 / Published online: 6 June 2024

Abstract

The scarcity of flat land in hilly areas has eventually forced geotechnical experts to utilize the sloping ground for construction purposes. The pleasant weather and attractive scenic views are the secondary reasons why there is a lot of infrastructure development taking place on hill slopes. In the last few years, a lot of attention has been given to the assessment of the bearing capacity of footing on hill slopes. However, due consideration has not been paid to the estimation of the bearing capacity of footings (width, B) on slopes, considering the consequences of earthquake shaking. In light of the foregoing, a comprehensive analysis has been conducted using a numerical tool based on the Finite Element Limit Analysis (FELA) to assess the ultimate seismic bearing capacity of footing on a c-ϕ slope and their potential failure modes, taking into account numerous parameters that control the aforementioned ones. The earthquake loading is considered by utilizing the pseudo-static approach. The influence of several parameters, specifically setback ratio (b/B), angle of internal friction of soil (ϕ), slope angle (β), horizontal seismic acceleration coefficient (α_h), and unit weight of soil (γ) on the ultimate bearing capacity of footing is studied. It is noted that the setback ratio and slope angle significantly impact the seismic load-bearing capacity, while the unit weight of the soil has minimal effect on seismic-bearing capacity. This study investigated the various potential failure modes of strip foundations resting on soil slopes under seismic loading.

Keywords Finite Element Limit Analysis (FELA) · Shallow foundations · Seismic bearing capacity · Strip footing · Slopes

List of symbols

B	Width of strip footing (m)
b	Distance of footing from the crest of the slope (m)
b/B	Setback ratio
q_{ult}	Ultimate bearing capacity of the footing (kPa)
γ	Unit weight of soil (kN/m^3)
E	Elastic modulus of the soil (MPa)
α_h	Horizontal seismic acceleration coefficient
ϕ	Angle of internal friction of soil (degrees)
β	Angle of soil slope with horizontal (degrees)
ν	Poisson's ratio
c	Cohesion of soil (MPa)

Introduction

The allure of scenic views has fuelled the infrastructure development and rapid urbanization in hilly regions, prompting extensive construction on slopes. Unlike flat grounds, foundations in these areas face heightened vulnerability to slope instability, a factor contingent on their proximity to the crest's edge. Furthermore, footings situated on slopes experience a significant reduction in ultimate bearing capacity compared to those on level ground. While prior studies suggest the possibility of safely neglecting this issue with a precise determination of ultimate bearing capacity, foundations on sloping sites remain susceptible to seismic activities. This susceptibility arises from topographical amplification of movement transmitted to the foundation base and a greater loss of strength due to incomplete mobilization of passive resistance toward the sloping side [1]. Post-earthquake site investigations and subsequent analyses underscore the severe stability problems that can arise in foundations, with a notable reduction in bearing capacity [2, 3]. Tatsuoka et al. [4] observed that, during earthquakes, structural failure

✉ Vinay Bhushan Chauhan
chauhan.vinaybhushan@gmail.com; vbcce@mmmut.ac.in

Nimisha Dwivedi
nimishadwivedi91@gmail.com

[1] Civil Engineering Department, Madan Mohan Malaviya University of Technology, Gorakhpur 273010, India

predominantly results from diminished load-bearing capacity rather than sliding or tilting.

Terzaghi [5] pioneered the initial approach to ascertain the ultimate load-bearing capacity of a foundation on level ground, a method still widely employed today. Subsequently, numerous researchers have delved into evaluating the ultimate bearing capacity of footings on horizontal ground [6–10], as well as their seismic bearing capacity on flat terrain [11–14]. Meyerhof [6] introduced a modified failure mechanism derived from Terzaghi, expanding the slip surface of the passive zone to the ground surface and devising a new expression for determining the factors influencing ultimate bearing capacity. Hansen [7] and Vesic [8] also proposed novel expressions for footing ultimate bearing capacity, incorporating factors related to shape, depth, and inclination. Earlier studies explored the impact of the horizontal seismic acceleration coefficient (α_h) on the seismic bearing capacity of footings on level ground [11, 12].

The existing literature highlights a predominant focus within current design codes on estimating the ultimate bearing capacity exclusively on flat grounds, offering limited guidance for buildings situated on hill slopes [15–19]. Furthermore, there is a notable absence of guidelines addressing the assessment of ultimate bearing capacity in the presence of seismic effects on slopes [20]. Studies pertaining to strip footing on hill slopes predominantly rely on methods such as stress characteristics [13], limit equilibrium [21], upper bound limit analysis [22], and the lower bound theorem of limit analysis [23]. Previous investigations underscore that seismic ultimate bearing capacity is significantly influenced by factors such as the setback distance of the footing from the slope crest (b), horizontal seismic acceleration coefficient (α_h), loading pattern on the footing, and slope inclination relative to the horizontal ground (β). Various factors, such as the soil shear strength parameters (specifically, cohesion and angle of internal friction), the relative density of the soil, and the depth of foundation embedment, exert influence on the ultimate bearing capacity of the footing. These factors collectively contribute to the overall bearing capacity of the foundation, particularly when situated on slopes [19, 23–25]. Despite the recognized importance of these key parameters, their cumulative effect on the response of hill-slope footings has not received adequate attention. Most analyses of footings on or along hill slopes in existing studies involve assuming a primary failure plane. However, with the advent of modern computational techniques like Finite Element Limit Analysis (FELA), which eliminates the need for such assumptions, the analysis of these complex geotechnical problems has become more accessible.

In light of the earlier discussion, it becomes imperative to determine the seismic ultimate bearing capacity of a footing situated on a slope. To achieve the objectives of this study, an in-depth numerical modeling employing adaptive finite element limit analysis is executed. The focus is on estimating the seismic bearing capacity of a strip footing positioned on a soil slope. Additionally, the study assesses the impact of various governing parameters to comprehend the extent of their influence on the seismic ultimate bearing capacity of foundations resting on slopes.

Furthermore, the analysis aims to evaluate the potential failure modes of strip footing on soil slopes, providing insights into the influence of different factors on these failure modes and the seismic bearing capacity of the footing.

Problem statement and methodology

The primary aim of this study is to assess the seismic bearing capacity of a strip footing situated on a slope with c-ϕ soil. It is widely acknowledged that hill slopes typically consist of various soil types, including gravels, fine silts, highly weathered rock masses, and soil mixtures. Hence, opting for c-ϕ soil for such slopes appears to be a fitting choice, both from a theoretical and practical standpoint. The constitutive model assumed for c-ϕ soil in this study is the elastoplastic model, specifically the Mohr–Coulomb failure criterion with an associated flow rule.

For a strip footing with width, B, situated on a c-ϕ soil slope with a unit weight of γ, the ultimate seismic bearing capacity (q_{ult}) can be formulated in terms of bearing capacity factors, as provided by past studies [5, 26].

$$q_{ult} = cN_{cs} + \frac{1}{2}\gamma BN_{\gamma q} \tag{1}$$

In Eq. (1), q_{ult} denotes the ultimate bearing capacity of the foundation, while N_{cs} and $N_{\gamma q}$ represent the bearing capacity factors under earthquake loading. This study operates under the assumption that the principle of superposition is applicable.

In this study, finite element limit analysis (FELA) is utilized using adaptive mesh techniques, employing 6-noded Gauss elements for the designated mesh of the numerical model. Plastically bound limit analysis theorems [27] guide this approach, which is widely employed for slope stability analyses under static and earthquake loading conditions, as evidenced by prior studies [28–30].

The 'Plate' element in the Optum G2 tool models the strip footing, exhibiting properties of a rigid material [31, 32]. The slope and footing geometry details are depicted in Fig. 1. The slope's angle of inclination with the horizontal varies from 20° to 40°, with the slope having a height of H. According to Boussineq's Elastic stress theory, the effect of the applied stress is considered negligible beyond the

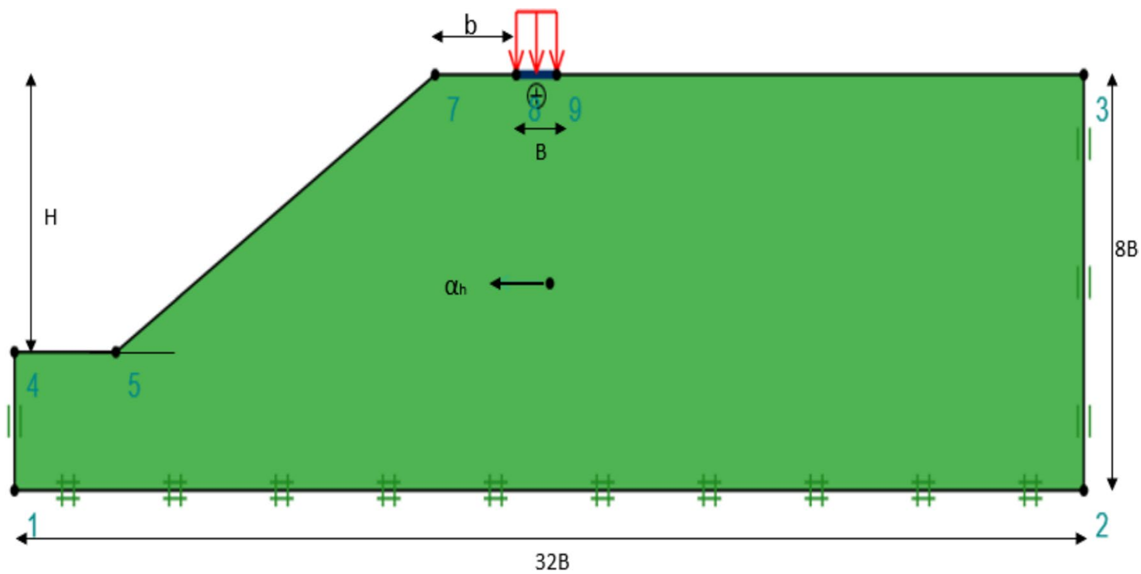

Fig. 1 Problem definition of an strip footing resting on the slope subjected to uniformally distributed load

"$0.1q_{ult}$" stress contour, represented as the outermost isobar. Figure 2 illustrates the chosen dimensions to ensure the isobar does not touch the boundaries of the model.

The domain size of the considered model is maintained sufficiently large to prevent the yielding of the soil mass around selected boundaries even after collapse. The base of the model restricts movement in both directions, while horizontal movement is constrained only for the right and left lateral boundaries. No restrictions are placed on movement along the inclined slope, allowing for free deformations under any loading. A multiplier-distributed load is applied to the strip footing, increasing from zero to the ultimate load at a uniform rate. To enhance the accuracy of the numerical simulation results, the total number of elements in the designated mesh is systematically adjusted, ranging from 5000 to 20,000 elements at intervals of 100 elements. It was observed that a mesh with 15,000 elements proved to be adequate for precise determination of seismic load-bearing capacity. Additionally, numerical models with a total number of elements exceeding 15,000 did not significantly affect the obtained q_{ult} [32].

Simulations are conducted to cover the validation of the numerical model, evaluation of seismic bearing capacity, and examination of the effects of varying governing

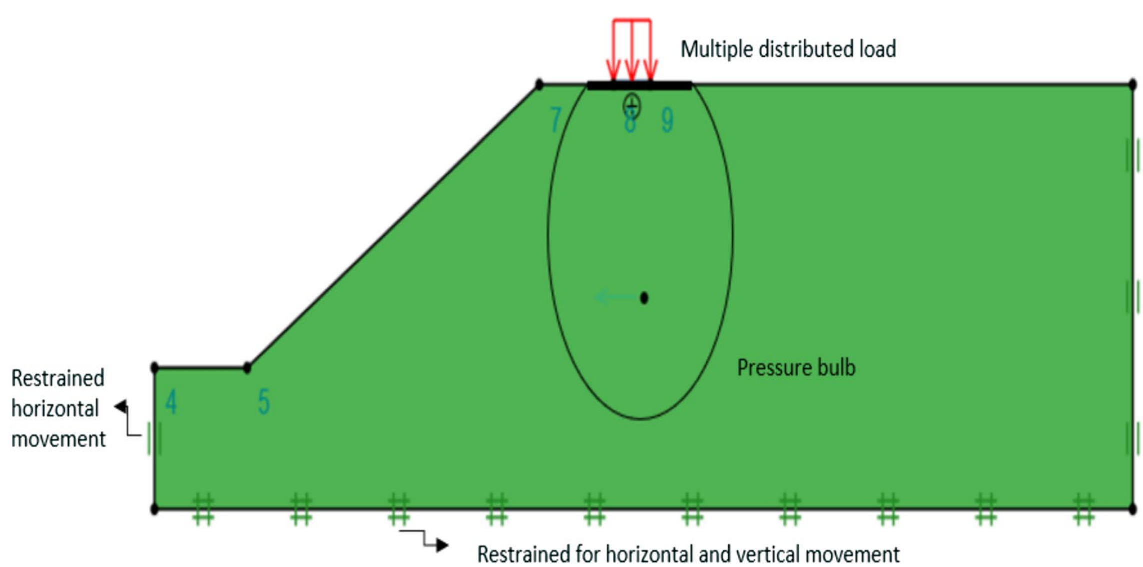

Fig. 2 Schematic representation of the plain strain model used for numerical simulation

parameters. These parameters include the angle of internal friction of soil, slope angle, setback distance, elastic modulus of soil, dry unit weight of foundation soil, and horizontal seismic acceleration coefficient (α_h).

Validation of the numerical model

To obtain precise results from the numerical model, a crucial step involves validating the developed model. To validate the numerical model employed in this study, a two-part validation process was undertaken. Initially, the ultimate bearing capacity of a strip footing resting on a slope under static loading was investigated. In the subsequent part of the validation study, the model was validated against a previous study that determined the seismic bearing capacity of a strip footing on a slope.

Bearing capacity of strip footing on slopes in static (α_h = 0) case

The present numerical model is validated with a former study carried out by Acharyya and Dey [33] where an analysis of the determination of the ultimate bearing capacity of a strip footing situated on a slope is carried out, taking into account various influencing parameters. The investigation focused on a strip footing with a width of 0.8 m placed at the top of the slope. Five setback ratios were employed in the study (*b/B* = 0, 0.5, 1, 2, and 3). Soil stiffness parameters, including modulus of elasticity (15 MPa) and Poisson's ratio (0.3), were considered constants. The numerical simulation study encompassed a range of parameters: (1) soil's angle of internal friction (30°–40°), (2) slope angle from the horizontal (30°–40°), (3) embedment depth ratio (0–1.5), (4) unit weight of soil (15–19 kN/m^3), and (5) elastic modulus of soil (20–90 MPa).

Similarly, a numerical finite element-based model was developed in the current analysis, with a focus on calculating the ultimate bearing capacity of a footing on a slope, as depicted in Fig. 3. A 2-dimensional finite element model illustrates the load-settlement behavior of a footing with a width, *B* m, positioned at a setback distance, *b/B* = 2, on the crest of the slope, following the approach reported by Acharyya and Dey [33]. The model adopts the Mohr–Coulomb failure criterion as described by Acharyya and Dey [33]. The results obtained exhibit nearly identical behavior, demonstrating good agreement between the previous findings and the developed numerical model. The analysis indicates that the numerical model presented in this study is well-suited for representing the response of foundations under similar conditions.

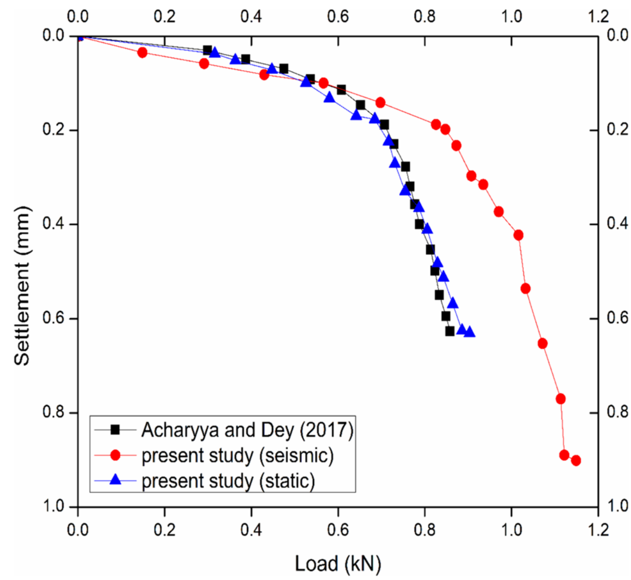

Fig. 3 Validation study: comparison of load settlement variation based on the present numerical model and study by Acharyya and Dey [33]

Table 1 Comparison of Q_{ult} of strip footing kept on unreinforced slope considering the effect of seismicity obtained from present analysis and available literature

Q_{ult} (Seismic bearing capacity, kN)				
α_h	Askari and Farzaneh [35]	Ausilo [34]	Halder and Chakraborty [36]	Present study Average of UB and LB limit analysis
0.1	202	241	202	223.5
0.2	169	203	169	197

Bearing capacity of strip footing on slopes considering seismic effect

In this segment the result obtained from the present study for seismic bearing capacity of strip footing on unreinforced slopes are compared with the available solutions of (1) upper bound limit analysis making logarithmic spiral failure by Ausilo [34]; (2) UB limit analysis making wedge failure by Askari and Farzaneh [35]; (3) LB limit analysis with a nonlinear program by Halder and Chakraborty [36]. Table 1 shows the comparison of previous studies from present study for the slope configuration with $\beta = 20°$; $\gamma = 0$; $\phi = 30°$; $c = 10$ kN/m^2 and *b/B* = 2. It is noticed that the UB results are in excellent agreement with the results of Ausilo [34] while the LB results of Halder and Chakraborty [36]. Also, it is noticed that the results obtained by Aksari and Farzaneh [35] are found to be a little lesser than the present UB solutions.

Results and discussions

After validation of the numerical model, a parametric study is done to analyze the effect of seismicity on footing considering geo-parameters. Also, the stability of footing on top of a slope is checked keeping setback ratio as one of the important parameters of the study. The different cases modelled based on the variation of parameters to estimate ultimate bearing capacity are presented in Table 2. Poisson's ratio (ν), the elastic modulus of soil (E), and cohesion are taken 0.3, 1300 MPa, and 50 kPa respectively as per reference [37, 38]. Five different setback ratios are taken in the study namely $b/B = 0$, 1, 2, 3, and 4. The results have been presented for $\beta = 20°–40°$, $\phi = 26°–34°$, $\alpha_h = 0.1–0.4$ g. Accordingly, the graphs and tables are provided for ultimate bearing capacity. It is to be noted that slope height H and footing width B were not varied in the present study.

Impact of setback distance (*b/B*)

The setback ratio is known to be one of the most significant governing parameters in the determination of the deformation and bearing capacity of a footing resting on a slope. A parametric study is performed to evaluate the influence of setback distance on 20°, 30°, and 40° slopes. In this case, $\nu = 0.3$, $\phi = 34°$, $\gamma = 17$ kN/m^3, $c = 50$ kPa and $E = 1300$ MPa were kept constant while multiplier distributed load was applied on the footing at each setback ratio (b/B) of 0, 1, 2, 3, 4, 5, 6 and 7. The variation of setback ratio with bearing capacity at different slope angles is shown in Figs. 4, 5, and 6. It is observed that for the slope of 20°, 30°, and 40° at $b/B = 0$, the q_{ult} is the least and as the b/B increases up to $b/B = 4$, 5, and 6, respectively, there is an increase in the bearing capacity. Other researchers [19, 38] have also reported a similar result compared to the results obtained in the present analysis. As a result, increasing the setback distance demonstrates an increase in the footing's carrying capability. Yang et al. [27] and, Naderi and Hataf [35] reported that the seismic bearing capacity of footing improves with a rise in the b/B ratio from the crest. Maximum (setback ratio) b/B within which there is a substantial influence on the bearing capacity of footing ranges from 1 to 5. Again, it should be noted that after the footing is placed at $b/B \geq 4$, 5, and 6 for slopes 20°, 30°, and 40°, respectively the effect of slope angle reduces to a larger extent and it

Table 2 Parameters of demonstrative cases

Case Details	β	α_h	γ (kN/m^3)	ϕ	b/B
Case I	20°	0.0 g, 0.1 g, 0.2 g, 0.3 g,0.4 g	17	34°	0, 1, 2, 3, 4, 5, and 6
Case II	30° and 40°	0.0 g, 0.1 g, 0.2 g, 0.3 g,0.4 g	17	34°	0, 1, 2, 3, 4, 5, 6, and 7
Case III	30° and 40°	0.0 g, 0.1 g, 0.2 g, 0.3 g,0.4 g	17	26°, 30°, and 34°	0, 1, 2, 3, 4
Case IV	20°, 30° and 40°	0.0 g, 0.1 g, 0.2 g, 0.3 g,0.4 g	15, 17, and 19	34°	0, 1, 2, 3, 4

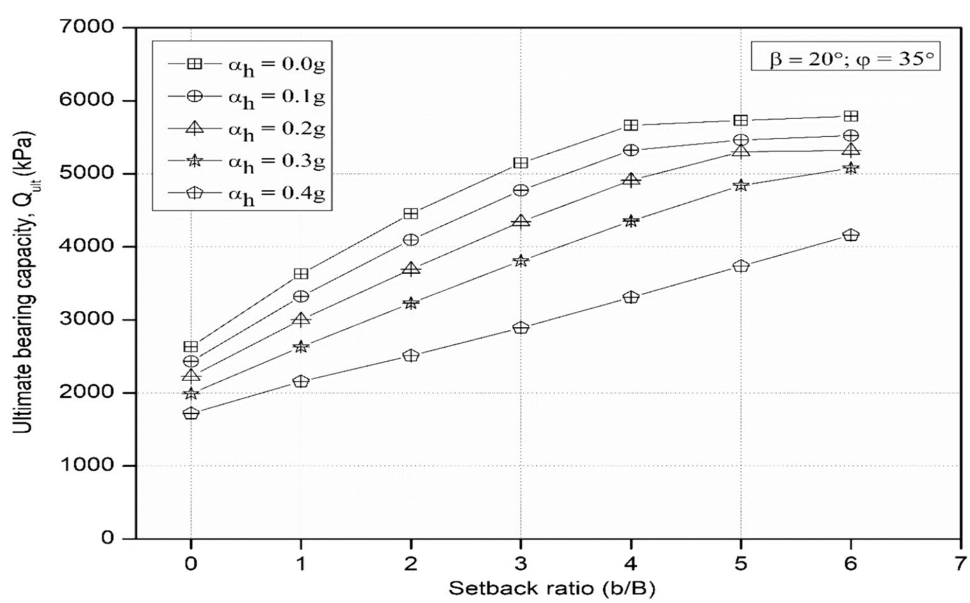

Fig. 4 Variation of q_{ult} with setback distance at $\beta = 20°$ for $\alpha_h = 0.0$ to 0.4 g

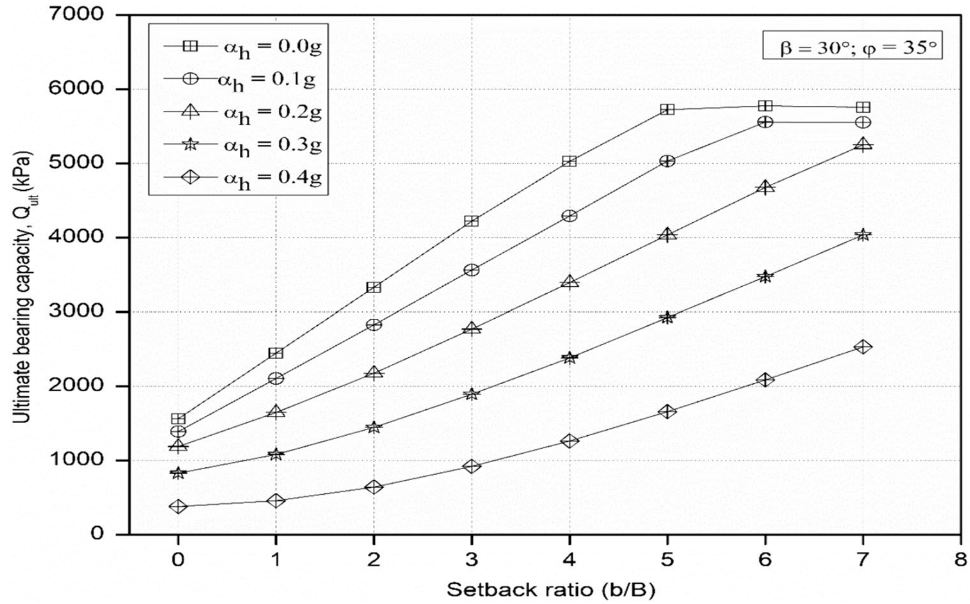

Fig. 5 Variation of q_{ult} with setback distance at $\beta = 30°$ for $\alpha_h = 0.0$ to 0.4 g

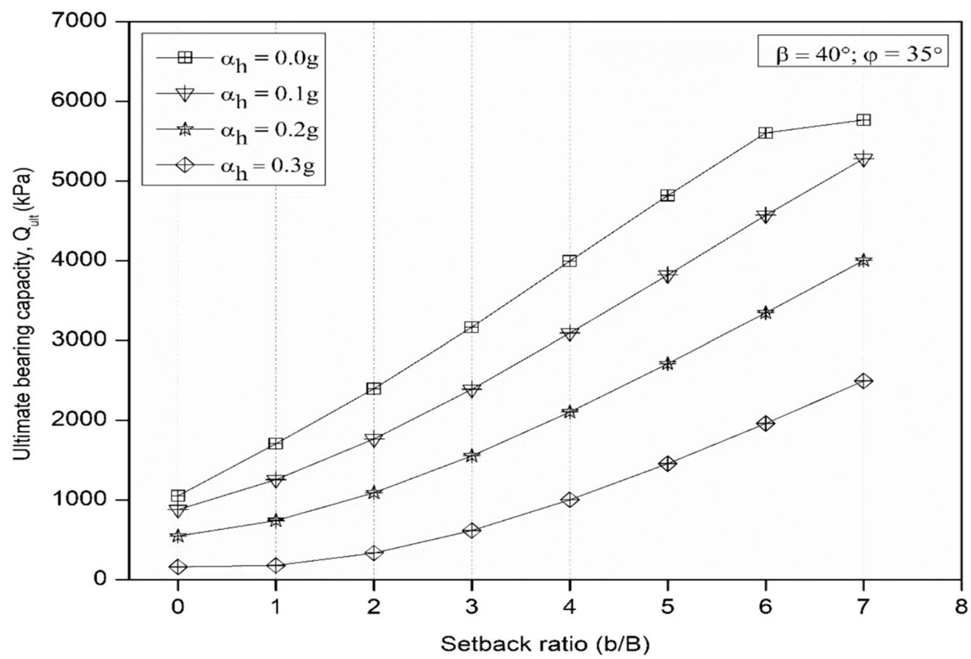

Fig. 6 Variation of q_{ult} with setback distance at $\beta = 40°$ for $\alpha_h = 0.0$ to 0.4 g

starts behaving as horizontal ground. Also, the study is done to see the effect of setback distance along with horizontal seismic coefficient varying from 0.1 to 0.4 g. And, it is found that with a rise in α_h bearing capacity kept on reducing. These variations can be because when the footing is kept at a lower setback ratio or when the footing is close to the sloping boundary it fails to provide enough passive confinement and any application of load results in the incomplete development of the resisting passive zone beneath the footing owing to less bearing capacity. The creation of the passive zones becomes more complete as the setback distance increases, limiting the foundation's lateral movement and preventing the loss of confinement, thus increasing bearing capacity.

Impact of slope angle (β)

To examine the effect of the slope angle β on the ultimate bearing capacity of footing having a width of B m, was positioned at each setback ratio of 0, 1, 2, 3, 4, 5, 6, and 7 in the 20°, 30°, and 40° slopes of height H m. The values of load put on the footing were taken from zero to ultimate load at a uniform rate. The variation of bearing capacity at different slope angles is shown in Figs. 4, 5, and 6. It is observed that seismic bearing capacity reduces as the slope angle increases regardless of the setback ratio. This result satisfies the findings of [23] who determined that the bearing capacity reduces with an increase in slope angles. It is observed that the stability conditions of the footing lying on the slope are significantly affected by an increase in slope angles. This points out the fact that the zone of passive resistance keeps on reducing as the slope angle increases and thus less resistance will be given by soil positioned towards the slope face towards failure.

Impact of horizontal seismic coefficient (α_h)

It is observed that variation of horizontal seismic coefficient (α_h) plays a major role in the determination of the bearing capacity of footing on slopes. It is to be noted that at lower slope inclination ($\beta = 20°$) when the horizontal seismic coefficient is increased from 0.1 to 0.4 g bearing capacity reduces in the range of 3700–2100 kPa for a *b/B* ratio of 2 which is lesser as compared to those at a higher inclination. Also, at higher inclination ($\beta = 40°$) the bearing capacity reduces drastically and ranges from 150 to 1050 kPa. Thus, a large gap can be seen in bearing capacity when α_h increased from 0.1 to 0.5 g at higher slope angles. This can be attributed to the fact that the angle of the active wedge right under the foundation grows greater as α_h increases, while the angle of a logarithmic spiral shear zone shrinks. Due to the action of seismic forces, the overall dimensions of the failure mechanism shrink as α_h increases, and the geometry of the failure mechanism moves laterally rather than vertically.

Impact of the angle of internal friction (ϕ)

This becomes an important parameter as it is the measure of the ability of soil to withstand shear stress. Thus, a parametric study is done to see the impact of ϕ on the footing of width *B* m which is kept at a setback ratio of 0, 1, 2, 3, and 4 at 30°, and 40° slopes. In this case, $\nu = 0.3$, $\gamma = 17$ kN/m^3, $c = 50$ kPa and $E = 1300$ MPa were kept constant while multiplier distributed load was given on the footing. Also, the horizontal seismic coefficient is varied from 0.1 to 0.5 g so that the effect of seismicity can also be studied. The angle of internal friction is varied in the range of 26°–34°. Figures 7 and 8 show the trend of variation of the angle of internal friction on the ultimate seismic bearing capacity.

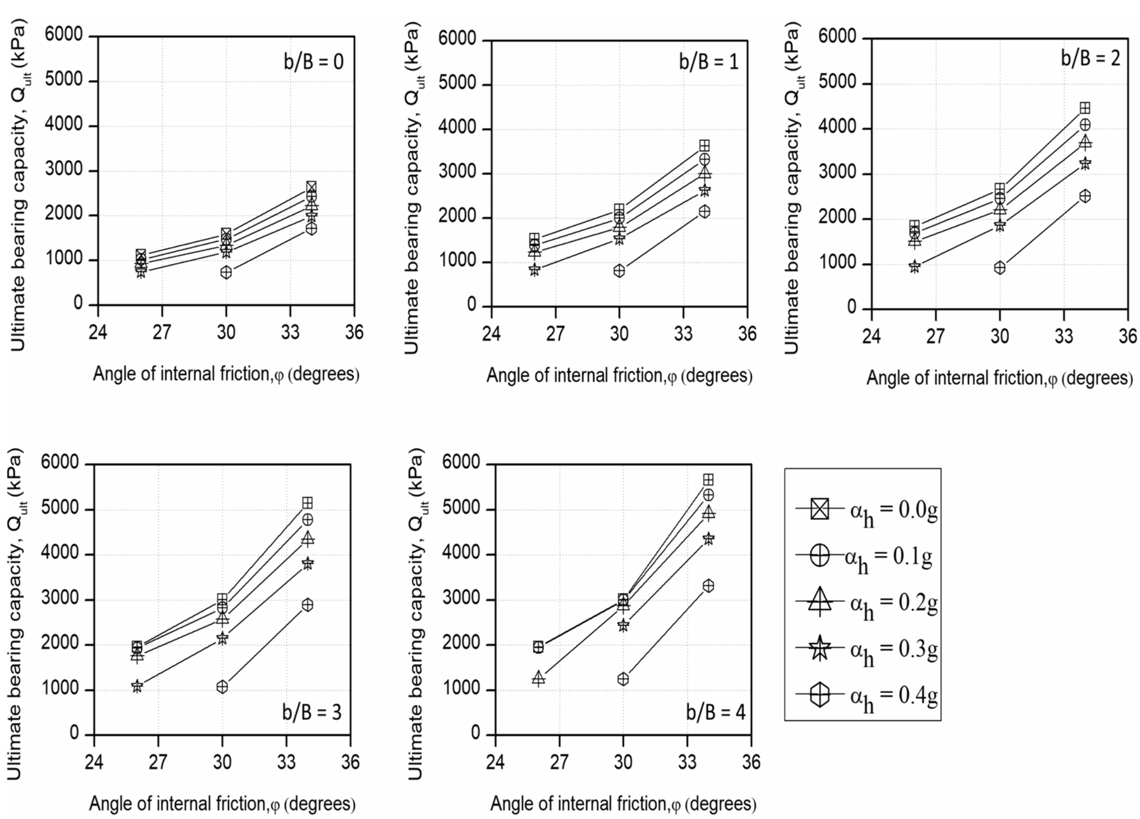

Fig. 7 Variation of q_{ult} with the angle of internal friction ϕ at setback distances (0–4) for horizontal seismic coefficients $\alpha_h = 0.0$ to 0.4 g at $\beta = 30°$

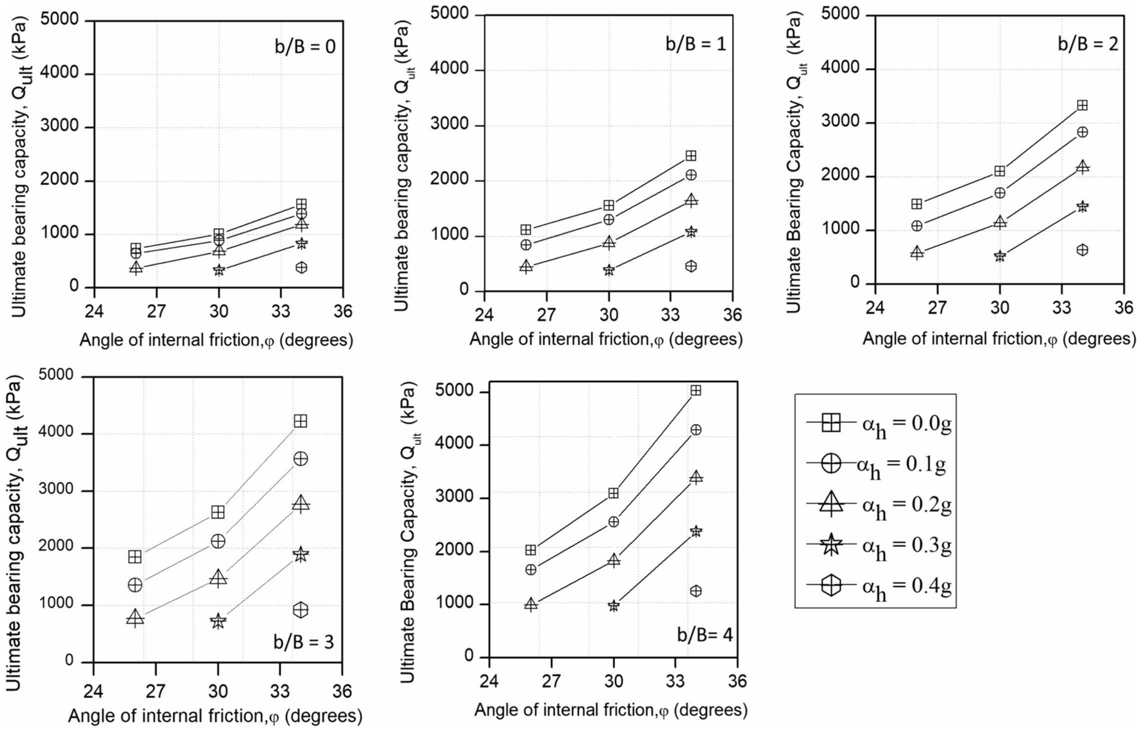

Fig. 8 Variation of q_{ult} with the angle of internal friction ϕ at setback distances (0–4) for horizontal seismic coefficients α_h = 0.0 to 0.4 g at β = 40°

So, it is noticed that ultimate bearing capacity improves with increasing ϕ from 26° to 34° due to the fact increase in ϕ leads to an increase in confinement between soil particles and hence an increase in the shear strength of the soil. Also, it is found that the collective effect of the angle of internal friction and setback distance has a noteworthy effect on the bearing capacity.

Impact of unit weight of soil (*γ*)

A parametric study is done to understand the impact of γ on the footing of width B m which is kept at a setback ratio (*b/B*) of 0, 1, 2, 3 and 4 at 20° and 30° slopes. In this case, ν = 0.3, ϕ = 30°, c = 50 kPa, and E = 1300 MPa were kept constant while multiplier distributed load was given on the footing to see the effect of unit weight of soil on the seismic bearing capacity. Unit weight of soil has been varied ranging from γ = 15 to 19 kN/m^3. Tables 3 and 4 show the variation of unit weight on normalized seismic bearing capacity at different setback distances with α_h ranging from 0.1 to 0.4 g. It is noticed that with the change in a unit weight of soil, no major significant effect on the bearing capacity of the soil was shown. Acharyya and Dey [34] have also reported a similar result when the variation of unit weight from 15 to 21 kN/m^3 in static conditions.

Failure mechanisms of footing on slopes

Figure 9 illustrates the plots of the potential failure plane of strip footing resting on unreinforced slopes showing the impact of setback distance (*b/B*) for the cases of α_h = 0.1 g with slope angle (β = 20°). As shown in for *b/B* = 0, a non-plastic triangular wedge under the strip footing is seen and the slip line reaches up to the sloping surface. When we increase the value of (*b/B*) to 1, 2, and 3 the depth of the failure zone surface keeps on increasing as the and slip line extends to the free sloping surface. Again, for the cases *b/B* = 4 *to b/B* = 5, i.e., the cases with higher values of *b/B,* it is noticed that the failure plane is not affected by the slope. Again, when the setback distance (*b/B)* is further increased to 6 it is noticed that the effect of the horizontal seismic coefficient has reduced, and also the bearing capacity failure is not influenced by the slope giving a failure plane similar to horizontal ground.

For comparison, Fig. 10 shows the influence of horizontal seismic coefficient α_h ranging from 0.1 to 0.4 g, and the plots of shear dissipation are shown in the figure for the cases β = 30° and *b/B* = 2. In the figure, when α_h = 0, a triangular zone is seen below the footing and the failure surface is extending to the sloping surface. When the value of α_h increases to 0.1 and 0.3 g the failure surface goes up to the sloping surface but the angle of the active wedge right under

Table 3 Impact of soil unit weight variations on bearing capacity of footing resting on 20° slope

Unit weight, γ (kN/m^3)	Setback ratio (b/B)	Normalized BC at $\alpha_h=0$	Normalized BC at $\alpha_h=0.1$ g	Normalized BC at $\alpha_h=0.2$ g	Normalized BC at $\alpha_h=0.3$ g	Normalized BC at $\alpha_h=0.4$ g
15	0	41.65	38.75	35.7	32.22	28.35
	1	56.63	52.2	47.33	42.03	35.53
	2	69.25	64.02	58	51.23	41.83
	3	79.75	74.3	67.83	60.1	47.83
	4	86.37	82.7	76.33	68.63	54.28
17	0	38.71	35.78	32.75	29.26	25.28
	1	53.37	48.85	44.15	38.69	31.71
	2	65.53	60.24	54.32	47.49	36.93
	3	75.71	70.22	63.9	56	42.51
	4	83.18	78.29	72.24	64.03	48.66
19	0	36.34	33.45	30.38	26.91	22.79
	1	50.62	46.34	41.42	35.92	27.99
	2	62.61	57.45	51.46	44.42	32.84
	3	72.28	66.93	60.63	52.71	38.3
	4	76.95	74.66	68.74	60.57	44.17

Table 4 Impact of soil unit weight variations on bearing capacity of footing resting on 30° slope

Unit weight, kN/m^3	Setback ratio, b/B	Normalized BC at $\alpha_h=0$	Normalized BC at $\alpha_h=0.1$ g	Normalized BC at $\alpha_h=0.2$ g	Normalized BC at $\alpha_h=0.3$ g	Normalized BC at $\alpha_h=0.4$ g
15	0	25.15	22.55	19.7	14.95	8.5
	1	38.6	33.43	27.35	19.08	10.15
	2	52.03	44.72	35.3	24.78	13.4
	3	65.32	58.87	44.47	31.67	17.93
	4	77.7	67.03	53.98	39.28	23.28
17	0	22.99	20.44	17.47	12.18	5.59
	1	36.03	30.91	24.29	15.9	6.71
	2	49.07	41.53	31.9	21.24	9.43
	3	61.93	52.56	40.57	27.81	13.49
	4	73.99	63.12	49.88	35.09	18.53
19	0	21.32	18.74	15.67	9.97	3.18
	1	33.96	28.62	21.76	13.3	3.72
	2	46.63	38.91	29.21	18.3	5.99
	3	59.22	49.46	37.68	24.59	9.78
	4	70.7	60	46.64	31.64	14.53

the foundation grows greater as α_h increases, while the angle of a logarithmic spiral shear zone shrinks. When the value of α_h is kept at 0.4 g, the triangular failure zone disappears and the failure surface extends till the toe of the slope, and a large slip surface is noticed towards the ground surface indicating overall slope failure when α_h increases to 0.4 g.

Figure 11 depicts the potential failure plane of footing resting on top of the sloping surface. And, it is showing the effect of different slope angles (β) for the cases of $b/B=2$ and $\alpha_h=0.1$ g. the slope angle has been varied from $\beta=20°$ to $\beta=40°$. From Fig. 11 it is noticed that for the models with small slope angles the failure surface extends till the sloping surface and collapse mechanism remain unchanged. For the higher inclination slope angles cases it is noticed that the slip surface extends to the toe of the slope and a rigid non-plastic triangular wedge is formed under the footing and the overall dimension of the failure mechanism has increased and a larger mass of soil fails. With the further increase in slope angle i.e., for the models with large values of β, the failure mechanism is significantly affected.

Based on the comparison of various potential failure modes of foundations resting over slopes, they are broadly

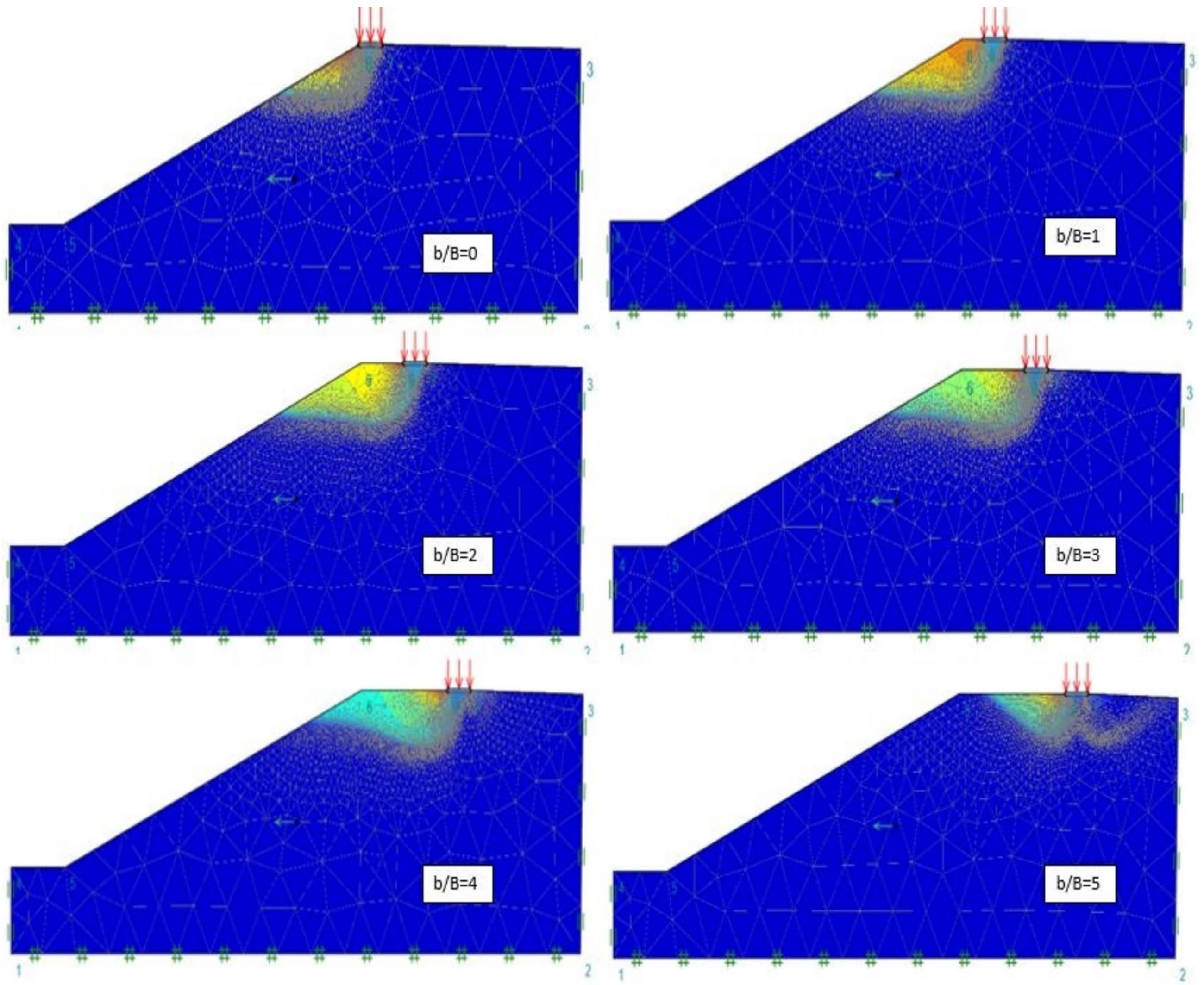

Fig. 9 Failure Pattern for $\beta = 30^{\circ}$ and $\alpha_h = 0.1$ g with *b/B* ranging from 0 to 5

categorized in different cases, which are summarized and presented in the Table 5.

Conclusions

The stability analysis of a strip footing resting on the crest of the *c*-*ϕ* soil slope has been evaluated by creating a numerical model with the main concern on seismic bearing capacity. A series of 2-D detailed parametric studies based on FELA is done to investigate the impact of the definite parameters on the ultimate seismic bearing capacity of footing. Also, the failure mechanism of the footing has been studied in detail. The major conclusions drawn from the study can be summarised below.

1. The setback ratio *b/B* increases the ultimate seismic load-bearing capacity of the footing for all the cases.
2. The ultimate bearing capacity of the footing (q_{ult}) resting over unreinforced soil slope up to a large extent. The improvement in bearing capacity ranges from 70

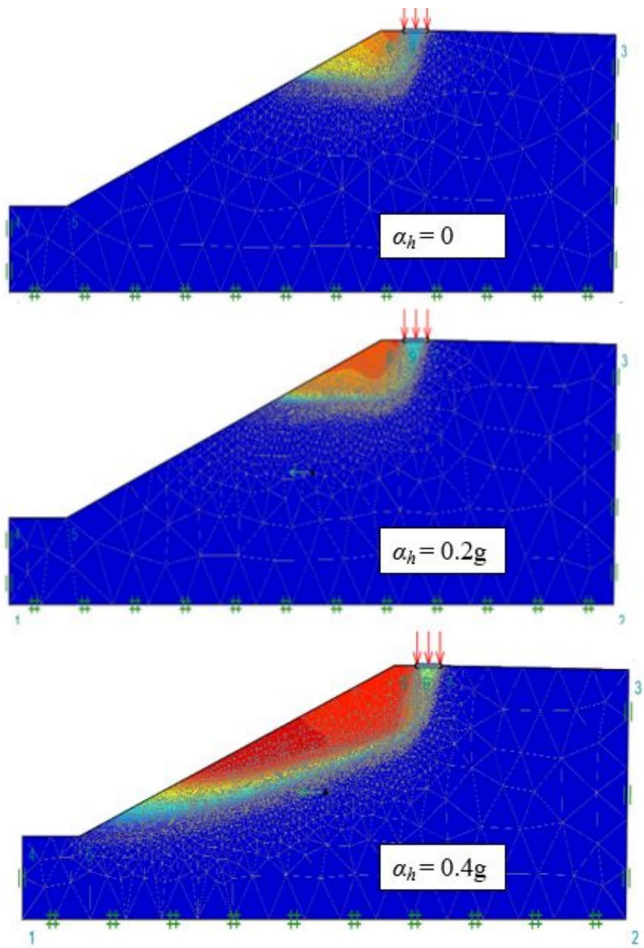

Fig. 10 Failure pattern for $\beta = 30°$ and $b/B = 1$ with varying α_h

to 80% with the increase in setback ratio. For slope 20°, 30°, and 40° increase in bearing capacity from $b/B = 0$ to $b/B = 6$ is approximately 2.1 times, 3.7 times, and 5 times respectively. For slope 20°, 30°, and 40° beyond setback ratios greater than or equal to 5, 6, and 7 respectively, seismic bearing capacity is not influenced much as it starts acting as flat ground.

3. In the case of strip footing kept at the crest of the slope, the value of seismic bearing capacity reduces with increase in the value of slope angle β as the zone of passive resistance keeps on reducing as the slope angle increases and thus less resistance will be given by soil positioned towards slope face towards failure.
4. The value of q_{ult} decreases with an increase in horizontal seismic coefficient α_h and a large gap can be seen when α_h is increased from 0.1 to 0.5 g at higher slope angles due to the fact that the angle of the active wedge right under the foundation grows greater as α_h increases, while the angle of a logarithmic spiral shear zone shrinks.
5. An increase in friction angle of soil ϕ improves the seismic bearing capacity and due to an increase in confinement between soil particles and hence an increase in shear strength of the soil.
6. An increase in the unit weight of soil has no major significant effect on the seismic bearing capacity of the soil. An increase in normalized bearing capacity is observed when b/B changes from 0 to 4 and a reduction in normalized bearing capacity is noticed when α_h changes from 0.0 to 0.4 g for all slope angles.

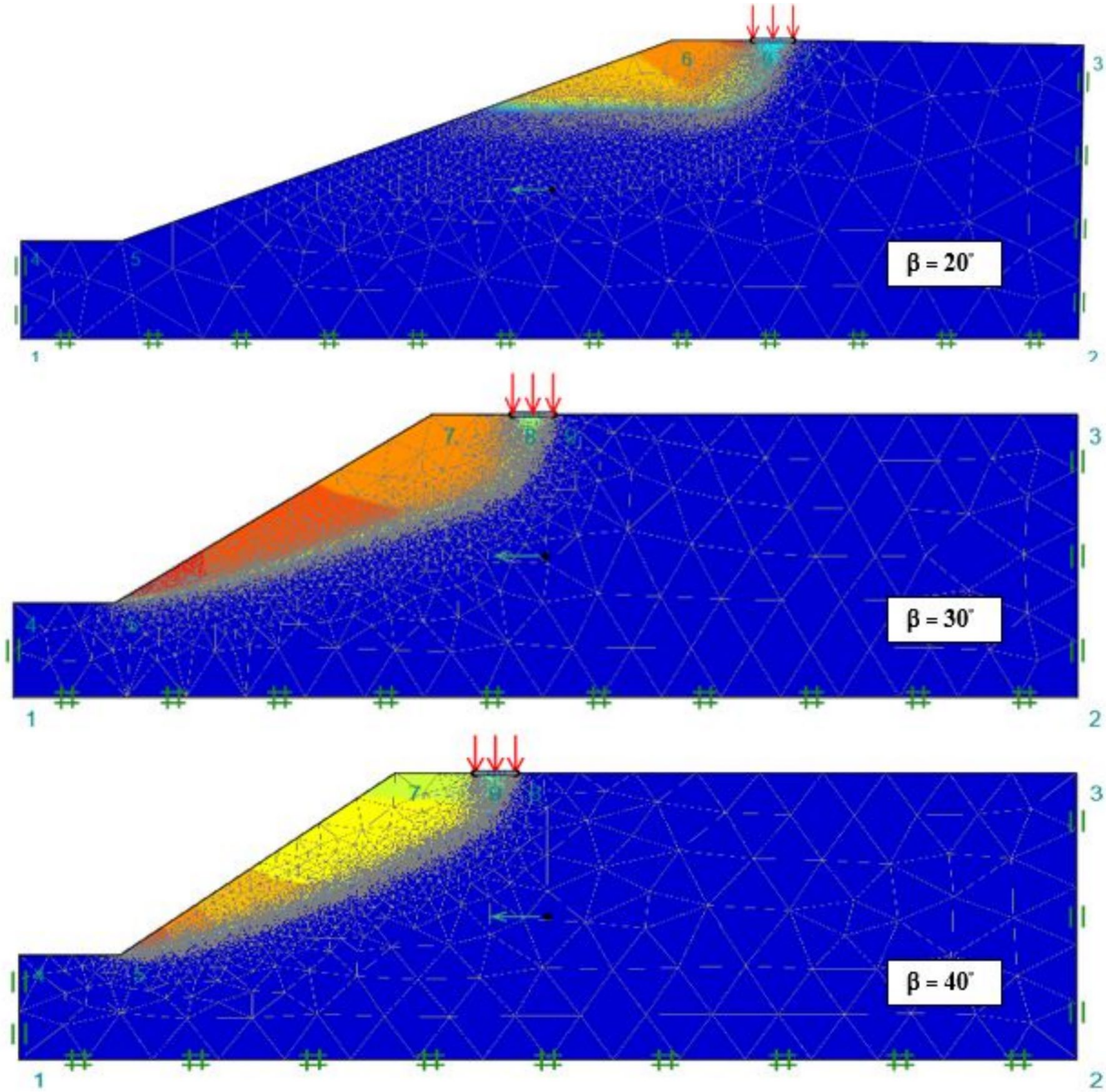

Fig. 11 Failure Pattern for $b/B = 2$ and $\alpha_h = 0.1$ g with slope angles (**a**) $\beta = 20°$; (**b**) $\beta = 30°$; (**c**) $\beta = 40°$

Table 5 Categorization of failure modes of foundations resting over slopes

Modes of failure	Detailed explanation	Cases
Type I	Failure plane developed within slope surface	1. $b/B = 1$, $\alpha_h = 0.1$ g, 0.2 g and 0.3 g for $\beta = 30°$ 2. $\alpha_h = 0.1$ g; $\beta = 20°$; $b/B = 0$, 1, 2, and 3
Type II	Failure plane extending till toe of hill-slope	1. $\beta = 30°$, $b/B = 1$ for $\alpha_h = 0.4$ g 2. $\beta = 30°$, and 40; $b/B = 2$ and $\alpha_h = 0.1$ g
Type III	Failure plane not influencing the slope	$\beta = 30°$, $\alpha_h = 0.1$ g for $b/B = 4$ and $b/B = 5$
Type IV	Complete slope failure	$\beta = 30°$, $b/B = 1$ for $\alpha_h = 0.5$ g

Acknowledgments None.

Funding Nil.

Data availability No data set is associated with the paper.

Declarations

Conflict of interest On behalf of all authors, the corresponding author states that there is no conflict of interest.

Ethical approval This article does not contain any studies with human participants or animals performed by any of the authors.

Informed consent For this type of study, formal consent is not required.

References

1. Dey A, Acharyya R, Alammyan A (2019) Bearing capacity and failure mechanism of shallow footings on unreinforced slopes: a state-of-the-art review. Int J Geotech Eng. https://doi.org/10.1080/19386362.2019.1617480
2. Huang C, Chen Y (2004) Seismic stability of soil retaining walls situated on slope. 130(1):45–5. https://doi.org/10.1061/(ASCE)1090-0241(2004)130:1(45)
3. Huang C, Kang W (2008) Seismic bearing capacity of a rigid footing adjacent to a cohesionless slope. Soils Found 48(5):641–651. https://doi.org/10.3208/sandf.48.641
4. Tatsuoka, F, Koseki J, Tateyama M, Munaf Y, Horii K (1998) Seismic stability against high seismic loads of geosynthetic-reinforced soil retaining structures, Keynote Lecture. In Vol 1 of Proc., 6th Int. Conf. on Geosynthetics, pp 103–142. Atlanta: International Geosynthetics Society
5. Terzaghi K (1943) Theoretical soil mechanics. John Wiley and Sons, New York, USA
6. Meyerhof G (1951) The ultimate bearing capacity of foundations. Geotechnique 2:301–332
7. Hansen JB (1970) A revised and extended formula for bearing capacity Danish Geotechnical Institute. Bulletin 28: 5–11
8. Vesic AS (1975) Foundation Engineering Handbook, ed. HF Winterkorn and HY Fang, Van Nostrand Reinhold Co., New York
9. Fedorovskii VG (2003) Bearing capacity of an eccentrically and obliquely loaded strip foundation on a weightless cohesive bed. Soil Mech Found Eng 40(5):161–172. https://doi.org/10.1023/B:SMAF.0000010109.35709.7b
10. Ghosh P, Choudhury D (2011) Seismic bearing capacity factors for shallow strip footings by Pseudo-Dynamic Method. Eighth International Conference on Case Histories in Geotechnical Engineering. Disaster Adv 4(3):34–42 https://doi.org/10.1061/9780784482100.002
11. Dormieux L, Pecker A (1995) Seismic bearing capacity of foundation on cohesionless soil. J Geotech Eng 121(3):300–303. https://doi.org/10.1061/(ASCE)0733-9410(1995)121:3(300)
12. Soubra A-H (1997) Seismic bearing capacity of shallow strip footings in seismic conditions. Proc Inst Civ Eng Geotech Eng 125(4): 230–241. https://doi.org/10.1680/igeng.1997.29659
13. Kumar J, Rao V (2003) Seismic bearing capacity of foundations on slopes. Geotechnique 53(3):347–361. https://doi.org/10.1680/geot.2003.53.3.347
14. Choudhury D, Rao S (2006) Seismic bearing capacity of shallow strip footings embedded in slope. Int J Geomech ASCE 6(3):176–184. https://doi.org/10.1061/(ASCE)1532-3641-(2006)6:3(176)
15. Shields D, Scott J, Bauer G, Deschenes J, Barsvary A (1977) Bearing Capacity of Foundation near Slopes. Proceedings of the 10th International Conference on Soil Mechanics and Foundation Engineering Japanese Society of Soil Mechanics and Foundation Engineering, Tokyo, Japan, 1: 715–720
16. Kumar SVA, Ilamparuthi K (2009) Response of footing on sand slopes. Indian Geotech Conf 77:622–626
17. Castelli F, Lentini V (2012) Evaluation of the bearing capacity of footings on slopes. Int J Phys Modell Geotech 12(3):112–118. https://doi.org/10.1680/ijpmg.11.00015
18. Keskin M, Laman M (2013) Model studies of bearing capacity of strip footing on sand slope. KSCE J Civ Eng 17(4):699–711. https://doi.org/10.1007/s12205-013-0406-x
19. Raj D, Singh Y, Shukla SK (2018) Seismic bearing capacity of strip foundation embedded in C-Φ soil slope. Int J Geomech ASCE. https://doi.org/10.1061/(ASCE)GM.1943-5622.0001194
20. Raj D, Singh Y, Kaynia A (2018) Behaviour of slopes under multiple adjacent footings and buildings. Int J Geomech ASCE. https://doi.org/10.1061/(ASCE)GM.1943-5622.0001142
21. Kumar J, Kumar N (2003) Seismic bearing capacity of rough footings on slopes using limit equilibrium. Geotechnique 53(3):363–369. https://doi.org/10.1680/geot.2003.53.3.363
22. Zhu, D (2000) The least upper-bound solutions for bearing capacity factor N_g Soils Found. 40(1):123–129. https://doi.org/10.3208/sandf.40.123
23. Chaudhary D, Rao S (2006) Seismic bearing capacity of shallow strip footings embedded in slope. Int J Geomech 6:176–184. https://doi.org/10.1061/ASCE1532-364120066:3176
24. Sarma SK, Chen YC (1996) Bearing capacity of strip footings near sloping ground during earthquakes, Proc of 11World Conference on Earthquake Engineering
25. Kumar J, Ghosh P (2006) Seismic bearing capacity for embedded footings on sloping ground. Geotechnique 56(2):133–140
26. Cheng YM, Lau CK (2017) Slope stability analysis and stabilization: New methods and insight, ISBN 9781138075504 Published April 28, 2017 by CRC Press 2nd Edition, Boca Raton, FL
27. Yang S, Leshchinsky B, Cui K, Zhang F and Gao Y (2020) Influence of failure mechanism on seismic bearing capacity factors for shallow foundations near slopes. Géotechnique 71(7):594-607. https://doi.org/10.1680/jgeot.19.P.329
28. Keawsawasvong S, Ukritchon B (2017) Undrained limiting pressure behind soil gaps in contiguous pile walls. Comput Geotech 83:152–158. https://doi.org/10.1016/j.compgeo.2016.11.007
29. Chowdhury R, Flentje P, Bhattacharya G (2010) Geotechnical slope analysis. CRC Press, Boca Raton, FL
30. Huang Y (2014) Slope stability analysis by the limit equilibrium method: Fundamentals and methods. ASCE Press, Reston, VA. https://doi.org/10.1061/9780784412886
31. Meyerhof GG (1957) The ultimate bearing capacity of foundation on slopes, Proceedings of 4th international conference on soil mechanics and foundation engineering, I, pp 384–386
32. OptumG2 (2020) Optum Computational Engineering, Copenhagen NV, Denmark
33. Pandey A, Chauhan VB (2020) Evaluation of pull-out capacity of helical anchors in clay using finite element analysis. In: Geocongress 2020: modeling, geomaterials, and site characterization, GSP 317, Minneapolis, Minnesota. American Society of Civil Engineers, pp 60–68. https://doi.org/10.1061/9780784482803.007
34. Ausilio E (2014) Seismic bearing capacity of strip footings located close to the crest of geosynthetic reinforced soil structures. Geotech Geol Eng 32:885–899. https://doi.org/10.1007/s10706-014-9765-4
35. Askari F, Farzaneh O (2003) Upper-bound solution for seismic bearing capacity of shallow foundations near slopes. Geotechnique 53(8):697–702. https://doi.org/10.1680/geot.2003.53.8.697

36. Halder K, Chakraborty D (2019) Effect of interface friction angle between soil and reinforcement on bearing capacity of strip footing placed on reinforced slope. Int J Geomech 19(5):06019008. https://doi.org/10.1061/(ASCE)GM.1943-5622.0002225
37. Acharyya R, Dey A (2017) Finite element investigation of the bearing capacity of square footings resting on sloping ground. INAE Lett 2(3):97–105. https://doi.org/10.1007/s41403-017-0028-6
38. Naderi E, Hataf N (2014) Model testing and numerical investigation of interference effect of closely spaced ring and circular footings on reinforced sand. Geotext Geomemb 42:191–200. https://doi.org/10.1016/j.geotexmem.2013.12.010